# Deep Construction Pit and Combined Pile-Raft Foundation for a High-Rise Building at the Red Sea

Alexander Mühl, Michael Brunner, Christian Wawrzyniak
CDM Smith Consult GmbH

A 260m tall high-rise building is to be built for a hotel complex in Jeddah, which is the pilgrims "gateway" on their pilgrimage to Mecca. The building ground consists of coralline limes stone of various formations. It is has largely preserved the unique skeletal structure of the coral reef which makes it very erratic. The groundwater level of the construction pit, which is located directly at the Red Sea, lies 10m above the excavation level. The Retaining and Shoring System consists of a diaphragm wall and a low-lying grouted sealing blanket. The foundation of the building is implemented by means of a three-meter thick reinforced concrete slab based on 125 large-diameter bored piles, which reach a depth of 50m.
The first paragraph of this article is dedicated to the geotechnical planning focusing on the application status of the FEM. The application and the effects of various soil models on the calibration of soil parameters and the modeling of piles by means of embedded piles will be discussed. The second section will describe the special production features regarding the low-lying grouted sealing blanket and the 50m deep piles in the coralline limestone. A special aspect is the use of micro-silica as additive to the bored pile concrete which is highly resistant to sulfate-bearing water.

## 1. Introduction

The "Kempinski Hotel & Residences," a project of the ASSILA Investment Company, will be located on the North Corniche of Jeddah about 100 m inland from the Red Sea. On 1,800 m² of the 9,600 m² sized property a high-rise building with 65 floors and 259 m height will be realized. The high-rise building will be founded on a 3 m thick raft slab with 2,900 m² area size and 125 piles.

**Figure 1** Kempinski Hotel & Residences, Jeddah, (www.perkinswill.com)

The foundation soil is composed of coralline limestone of widely varying strength, as well as silty sand derived from this formation. The coralline limestone has largely preserved the unique skeletal structure of the coral reef which makes it very erratic. Apart from its varying strength, the coralline limestone is characterized by irregular cavities, which pose a special challenge to the foundation of the high-rise building.

**Figure 2** Coral Rock Drill Core

In the first construction phase, the building pit for the three basement floors had to be built. The shoring system consists on a 400m long and 20m deep, single-layer anchored diaphragm wall and a low-lying grouted sealing blanket with a planned thickness of 4m. The grouted sealing blanket serves to reduce the groundwater inflow from 9000m³/h to remaining 1,800m³/h, which was discharged to the Red Sea via 30 deep wells and two discharge lines with a diameter of 800mm.

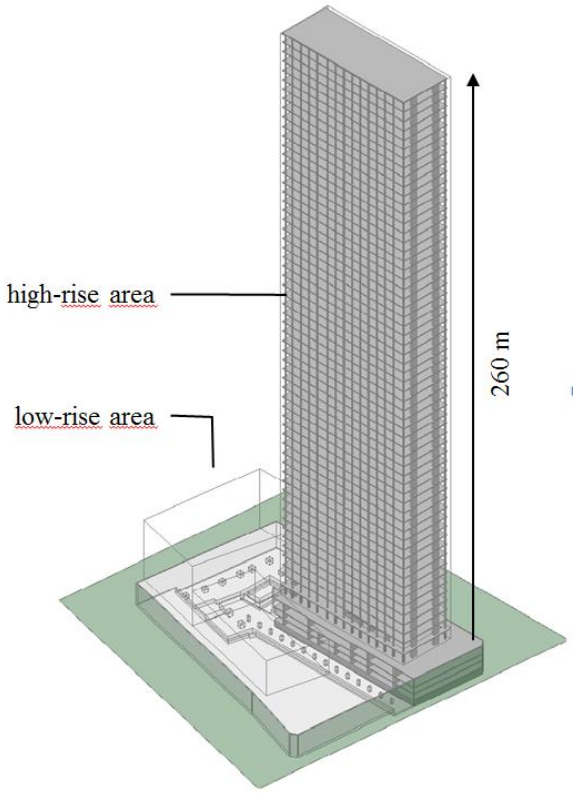


## 2 Foundation Design - Combine Pile-Raft Foundation

For the structural design a linear static analysis of a 3D-structure was performed. In this Model the tower foundation is considered as linear-elastic by the application of spring bearing supports. The stiffness of the spring bearings have been defined in result of numerical analyses using a 3D-Finite-Element-Model, in which soil, piles and raft slab are modeled with first order solid elements of hexahedra (brick) shape. To estimate the influence of cavities on the bearing behavior of the piled raft an element cluster with lower stiffness has been modeled below the base of a group of piles.

The numerical analyses were performed in the early stage of the design. The Structural Designer applied lowest and highest pile stiffness, while the position of the piles was adopted to optimize the distribution of forces iteratively by running several calculation processes, which lead to changes in the size of the raft slab and the number of piles. The diameter of piles of the high-rise building was amended in the tender phase from 1200mm to 1500mm to meet the client's need for safety. Neither the structural nor the geotechnical calculation was adjusted.

Difficulties in the production of the piles caused the company to question the static and geotechnical calculations. In this context, it needs to be mentioned that according to the contract (FIDIC) the company carrying out the building work in the next project phase is obliged to check the static calculations. After that it has to assume the warranty for all the planning and static calculations. In order to hand over a complete resilient design the analysis had to be revised. As the existing FE-Model was extremely simplified and the adjustments would have been very time-consuming we decided to create a completely new model. For this purpose, we used the calculation program of Plaxis bv. Plaxis 3D-V2012. Soil and structure are modelled by means of 10-node tetrahedral elements. This type of element provides a second-order interpolation of displacements. To obtain the force, the stiffness matrix and the mass matrix of the tetrahedral elements are integrated with four integration points. The quality of the 10-node element is comparable to a 20-node brick element.

The direct three-dimensional continuum finite element modelling is computationally very expensive. Some simplifications have been made to enable us to simulate the complex pile interaction, and the interaction between soil and structure. Instead of modelling 267 foundation piles by solid elements piles have been modelled as embedded piles. The embedded pile option has been developed to describe the interaction of a pile with its surrounding soil. The interaction at the pile skin and at the pile foot is described by means of embedded interface elements. The pile is considered as a beam which can cross the 10-node tetrahedral element at any place with any arbitrary orientation. Due to the existence of the beam element three extra nodes are introduced inside the 10-node tetrahedral element. In order to ensure that a realistic pile bearing capacity as specified can actually be reached, a zone in the soil volume elements surrounding the embedded pile is identified as elastic zone. The size of this zone is determined equivalent to the pile's radius. The elastic zone makes the embedded pile behave almost like a volume pile.

A 3D-CAD model representing the structural elements of the basement floor relevant for the load transfer was created for the implementation of the foundation structure. (**Fehler! Verweisquelle konnte nicht gefunden werden.**). The 3D-CAD model was integrated in PLAXIS and meshed.

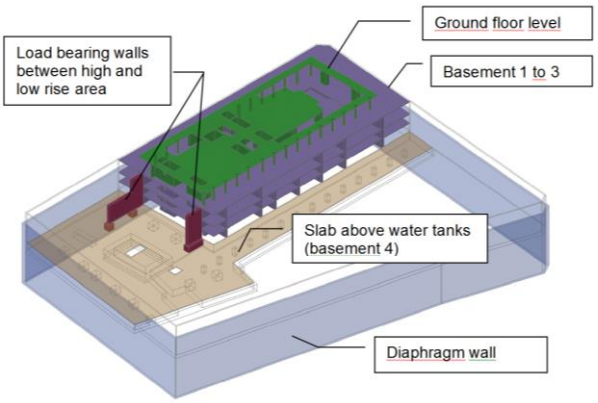


**Figure 3** Structural Elements of the Model

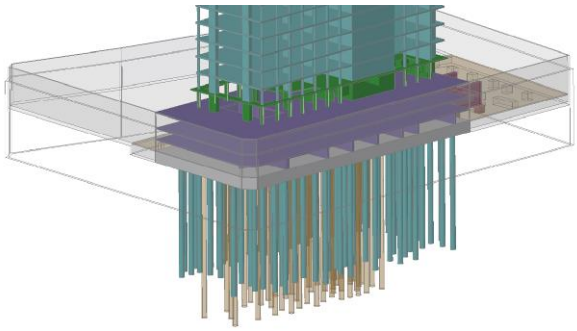

**Figure 4** Pile Foundation in the Area of the High-Rise Building

For the analysis the designer of the high-rise building handed over the data of the loads of the walls on the ground floor slab (see Figure 5).

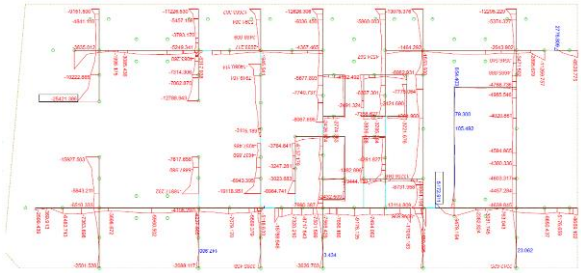

**Figure 5** Design Load at the Level of the Bottom Slab

Due to the irregular distribution of the line loads this level was not the appropriate interface level for applying the loads. We therefore searched an interface, which provided a comprehensive load image and decided in favor of the ground floor. Due to the distribution of pillar and wall loads on this floor (Figure 6) the load input became significantly easier. The basement floors and the ground floor were taken into account in the calculation by modelling them with volume elements with a linear-elastic stress strain behavior.

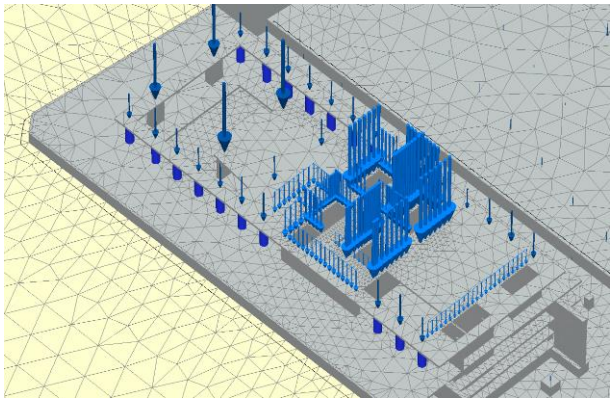

**Figure 6** FE Model - Area of High-Rise Building

To determine the load-bearing behavior of the piles three pile load tests were conducted by means of the Osterberg method.


**Figure 7** Osterberg Cell (Source: Prof. Dr.-Ing. E. Vees und Partner Baugrundinstitut)

In order to model soil parameters with the given results from this pile load tests a smaller 3D-FE-Model has been set up in PLAXIS. The test pile has been modeled as embedded pile. The skin resistance of the embedded pile element has been generated as function related to the strength properties of the soil in which the pile is located. Using this approach the pile bearing capacity is based on the stress state in the soil. The test piles showed no or hardly any pile base resistance, which is not exceptional for a heterogeneous coralline limestone. The pile base resistance was therefore set to zero.

Besides the Mohr-Coulomb model (MC-Model) what considers a linear-elastic, ideal-plastic material behavior the Hardening Soil Model (HS-Model) and the Hardening Soil Model with Small Strain Stiffness (HSsmall-Model) have been studied for the calibration. The Hardening Soil Model (HS-Model) considers a hyperbolic stress-strain relationship between the axial strain and the deviatoric stress in primary triaxial loading. For unloading-reloading stress path a linear elastic stress-strain relationship is used. The HSsmall-Model uses the same formulation as the HS-Model, but considers in addition the stiffness of soils at very small strains with a simple hyperbolic law.

At this point it has to be noted that the PLAXIS code and its soil models have been developed to perform calculations of realistic geotechnical problems. In this respect PLAXIS can be considered as a geotechnical simulation tool. The soil models can be regarded as a qualitative representation of soil behavior whereas the model parameters are used to quantify the soil characteristics. The simulation of reality remains an approximation, which implicitly involves that all soil models

do have their limitations. For the here defined task the MC-Model seems to be sufficiently applicable. For simplification it can be assumed that the coralline limestone does show a linear elastic stress strain behavior. The shape of the load-displacement curves obtained by back analysis in a 3D-FE-Model was in good accordance with the load-displacement curves obtained by the pile tests. For the MC-Model the shaft resistance, which is defined by $\tau_f = \sigma_n \cdot \tan \varphi + c$, is increasing more or less linear up to its peak. As the base resistance is neglected by our definition the pile is yielding at this point. Using the MC-Model results in underestimating the pile shaft resistance and the pile, which only sustains due to friction in the 3D-FE-Model, behaves softer. While $\sigma_n$ is nearly constant for the MC-Model it is increasing for the HS- and HSsmall Model. This increase is due to the deviatoric and volumetric hardening which these advanced models provide. That means in consequence calibrating soil parameters with a pile load test by the use of the MC-Model results in soil stiffness and shear strength higher than expected in reality. In a combined pile-raft foundation in which the raft transfers a greater proportion of the vertical load or sections of the raft are less supported by piles, the result of the FE calculation could underestimate the settlement and overestimate the reliability of the load-bearing capacity. Therefore, it must be analyzed if plausible results can be achieved for the load-bearing capacity of the raft with the calibrated parameters even without foundation piles.

Table 1 Calibrated Material Parameters

| Material Model | | | MC | HS | HSS |
|---|---|---|---|---|---|
| Unit weights | $\gamma_{sat}/\gamma_{dry}$ | [kN/m³] | 19/19 | 19/19 | 19/19 |
| Stiffness (Youngs Modulus at depth of 30 m) | E | [MN/m²] | 280 | 175 | 80 |
| Oedometer stiffness | $E_{oed}$ | [MN/m²] | 336 | 210 | 96 |
| Shear modulus | G | [MN/m²] | 112 | 70 | 32 |
| Cohesion | c′ | [kN/m²] | 150 | 85 | 85 |
| Internal friction | φ′ | [°] | 35 | 35 | 35 |
| Dilatancy angle | ψ | [°] | 0 | 0 | 0 |
| At rest lat. pressure coefficient | $K_0$ | [-] | 0.426 | 0.426 | 0.426 |
| Poisson's ratio | ν | [-] | 0.25 | 0.25 | 0.25 |
| At rest lat. pressure coefficient for NC | $K_0^{NC}$ | [-] | | 0.426 | 0.426 |
| Effective vertical stress at depth of 30 m | $\sigma_1$ | [kN/m²] | | -300 | -300 |
| Reference stress for stiffenes | $p^{ref}$ | [kN/m²] | | 100 | 100 |
| Power for stress-level dependency of stiffness | m | [-] | | 0.5 | 0.5 |
| Tangent stiffness for primary oedometer loading | $E_{oed}^{ref}$ | [MN/m²] | | 152 | 69 |
| Secant stiffness in standart drained triaxial test | $E_{50}^{ref}$ | [MN/m²] | | 152 | 69 |
| Unloading-reloading stiffness | $E_{ur}^{ref}$ | [MN/m²] | | 456 | 207 |
| Poisson's ratio for unloading-reloading | $\nu_{ur}$ | [-] | | 0.2 | 0.2 |
| Dynamic soil stiffness | $E_0^{ref}$ | [MN/m²] | | | 1035 |
| Reference shear modulus at very small strains | $G_0^{ref}$ | [MN/m²] | | | 431 |
| Shear strain at witch is $G_s = 0.722G_0$ | $\gamma_{07}$ | [-] | | | 1E-4 |
| Tensile strengh | $\sigma_t$ | [kN/m²] | 0 | 0 | 0 |
| Overconsolidation ratio | OCR | [-] | 1 | 1 | 1 |
| Interface stiffness ratio | $R_{int}$ | [-] | 1 | 1 | 1 |

The excavation of the 10m deep construction pit was another aspect speaking in favor of the HS- and/or HSsmall-Model. The MC-Model does not take into account a stress-depended stiffness. Accordingly the calculations with unloading due to excavation result in large heaves. Calculations with loads applied from the building result in large settlements.

The HSsmall model was favored as a result of the calculations. When using the MC- and/or HS-Model, settlements occurred in the area of the raft of the podium outside the foundation of the high-rise building, which are mainly characterized by heave. This is related to the accumulation of strains in areas of the model with small changes of stress, which are avoided in the HSsmall-Model by taking into account a higher stiffness at small strains.

The approach of modeling and calculating the foundation is described comprehensively in [L1].

The calculation results show, that the piled raft foundation provides sufficient capacity under vertical loading in the ultimate limit state (ULS). The calculated overall settlements and differential settlements, both within the high-rise area, and between the high-rise and low-rise areas are small and are within the limits of the serviceability limit state (SLS).

To investigate the influence of open cavities as well as sediment filled cavities element clusters of very low stiffness (0.1 MN/m²) have been modelled at different positions below pile groups of the piled raft foundation in the high-rise area. The ground floor areas of the element clusters have sizes of around 100 m² to 200 m². The thickness is 5 m. The element clusters are activated in the first calculation phase, whereas clusters beneath the 30m long piles are combined with clusters below the 40m long piles. 13 cluster combinations were analyzed (Figure 8 and Figure 9).

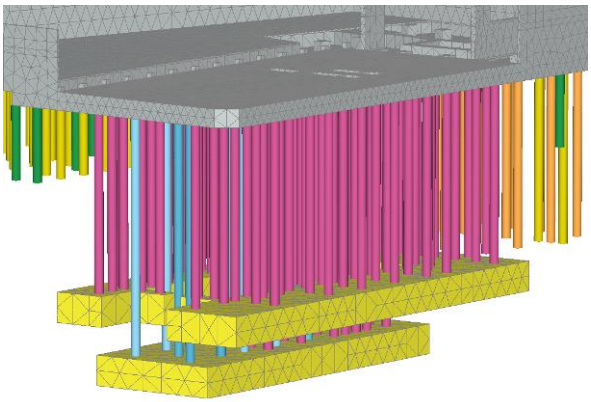

**Figure 8** FE-Model with Element Clusters

The result of the analysis showed that the load-bearing and deformation behavior of the combined pile-raft foundation is not significantly influenced by cavities in the area of the pile base. The raft can provide redundancy to the piles, for example, in case a group of piles is defective or weaker, or some pile groups encounter zones of cavities. Under these circumstances, the presence of the raft allows measure of re-distribution of the load from the affected piles to those that are not affected, and thus reduces the potential influence of pile "weakness" or influence of cavities on the foundation performance.

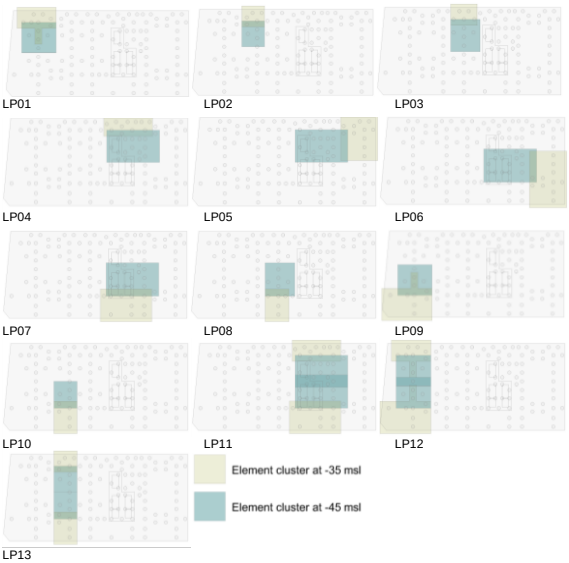


**Figure 9** 3D CAD Model with Cluster Combinations

## 3 Design - Retaining and Shoring System

The Retaining and Shoring System was designed by a subsidiary of the Italian company TREVI Spa., the ARABIAN SOIL CONTRACTORS. American standards form the basis for the design. Static forces were exclusively determined with the help of FE-Models. The coralline limestone was represented by using the MC-Model. We used the HSsmall-Model for our comparative calculations. Additionally, conventional analytical calculations for the design for safety against uplift and hydraulic failure of the base of the construction pit were also performed. The groundwater flow and the corresponding pore-water pressure distribution as input values of the analytical calculation were calculated in 2D- and 3D-FE-Models.

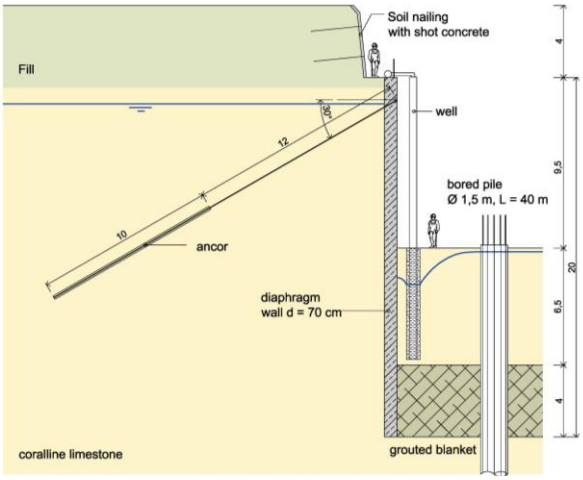


**Figure 10** Cross-Section of the Revetment

## 4 Ensuring the durability of Bored Pile Concrete

Due to the chemical environment in the soil, a high resistance against chloride and sulfate attack was required [L2]. As described in the tender documents, the concrete had to ensure the requirements of the exposure classes S3 and C2 according to ACI 318M-08 which is comparable to the exposure classes XA3 and XS2 according to DIN EN 206. The concrete mixtures available in Saudi Arabia are produced according to ASTM specification; however, concrete plants there are not able to supply concrete with predetermined exposure classes. The executing company had to choose a recipe that provides both a high chloride and high sulfate resistance. According to testing laboratories and suppliers, good results were achieved by the addition of microsilica in combination with Portland cement along the Saudi West Coast. Due to the higher tricalcium aluminate content (C3A) of Portland cement CEM I, it offers the better chloride resistance [L3] as opposed to the more sulfate constant CEM V (high content of slag sand). By the addition of microsilica the sulfate resistance should also be improved. For the pile concrete with a compressive strength class of $f_c$=35N/mm² a recipe with w/c =0.4 and 10% micro silica was chosen. Thus, the requirements for exposure class C2 according to ACI318M-08 were reached. Based on the laboratory results of the 3rd party, the chloride permeability was determined as "very low" according to the ASTM C1202 standards, thus a sufficient chloride resistance were confirmed.

According to ACI318M-08, the sulfate resistance can be determined in accordance with ASTM C 1012. Here rectangular test blocks with a length of 250 mm are stored in a solution of sulfate acid. For the exposure class S3, the storage time is 18 months.

In accordance with ACI318M-08 a maximum elongation for the exposure class S3 is 0.1% within this time frame. After 15 weeks an average increase in length of the sample bodies was determined at 0.012%.

In December 2013, after an 18 month storage period, an average length increase of 0.047% was determined. The maximum allowed longitudinal extension was not reached. The concrete mix used fulfills the requirements for exposure class S3.

**Figure 11** Sulfate test according to ASTM C1012, Test Blocks

## 5 Construction

### 5.1 Pile Construction

After the site clearing, piles with diameters of 60, 80 and 150 cm were to be constructed in approximately 10m above the excavation base. The lengths of the piles ranged from 14.5m and 40 m, so that drilling depths of up to 50 m were required. The drilling was carried out with a Soilmec SR70 and SR100.

**Figure 12** Pile Construction, Drilling Work

The first few meters of the drillings were supported with casing. The rest of the drilling was slurry-supported using polymer suspension.

**Figure 13** Installation of the casing

The reinforcement cages were constructed on site. Binding wire was mainly used for the fastenings. The 30m and 40m long cages, with weights of 4.7 to 10.1 tons, were installed in segments and then coupled together with clamps.


**Figure 14** Construction of Reinforcement Cages

Particularly difficult were the sediment-filled cavities and trenches in the coralline limestone that were encountered. Despite careful operation and the use of support liquid, the sediments have been "washed-out" due to drilling process. To avoid these voids reaching large sizes and collapsing, they were filled with sand cement as preventive measure and the drilling was continued later. In addition to the geologically-related difficulties, there were also problems with the cement delivery which had a negative impact on the work performance.

In addition to the chloride and sulfate resistance tests already discussed, the quality assurance also included compressive strength and fresh concrete tests (slump and temperature).

**Figure 15** Test Cylinders out of Bored Pile Concrete

Additionally, caliber tests, integrity test and cross-hole-sonic-tests as well as six Osterberg tests were performed.

**Figure 16** Bore Piles in the Area of the High-rise foundation

### 5.2 Construction of the Diaphragm Wall

The diaphragm wall with a wall thickness of 70cm and a depth of 20m was constructed by the two-phase method: the trench was excavated, to the full depth under a polymer-slurry, by clamshell and hydromill. Once the element was fully excavated, the reinforcement cage was installed and the concrete placed by tremie method. The selected type of polymer is resistant against the salty water environment. The polymer content was about 0.1 - 0.5%. The density of the fresh (sole) polymer mud is almost equal to that of water, or even slightly lower, because of air entrapment that can occur during mixing. Therefore, when only polymer is used to prepare the excavation slurry, the mud density cannot be a useful parameter for determining and controlling the dosage of the polymer. Depending on the situation, the bentonite content was between 2% and 5% and led to a Marsh viscosity of > 33s / l.

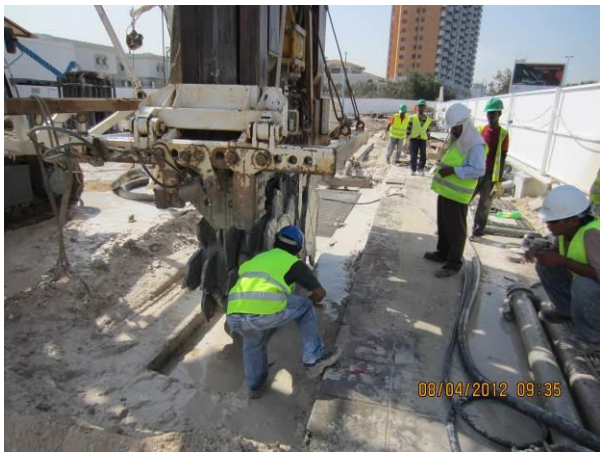


**Figure 17** Construction of the Diaphragm Wall

The construction of the diaphragm wall lent itself very well under the prevailing ground conditions. During excavation of the construction pit, mostly good quality wall surfaces were observed. Analogous to the pile cages, the reinforcement cages of the diaphragm wall were also pre-constructed on site.

**Figure 18** Diaphragm Wall during Excavation

### 5.3 Grouted Sealing Blanket

The sealing blanket was constructed to reduce the permeability of the coralline limestone in order to decrease notably the water inflow from the bottom of the excavation to ≤ 2.000 m³/h. In principal, the sealing blanket was constructed by permeation grouting, through Multi Packer Sleeved Pipes (MPSP), under controlled pressure. The method consists in dividing the entire hole in sections, separated by permanent packers: the grouting is performed through the steel pipe, equipped with rubber valves and bag-packers. The grid of MPSP consisted of a total of 3,200 grouting holes in a square-triangular pattern with a final distribution of about one hole each 3.12 m².

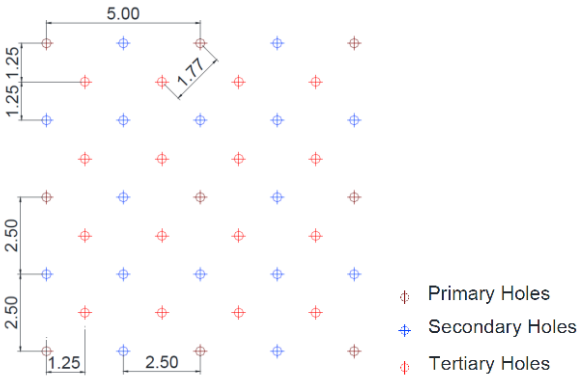


**Figure 19** Grouting Pattern

The grout was a Bentonite-Cement suspension with a cement/water ratio of C/W = 0.5 to 0.35 and a bentonite/water ratio of B/W = 0.03 to 0.05. The composition of the grout mixes has been defined by preliminary trial tests, carried out on samples. In addition to the refusal criteria of pressure and flow rate, a maximum grout take was set for the primary and secondary holes, which had to be increased at the beginning of the work. The tertiary holes were grouted with no limit of grout take. The refusal criteria were led by pressure.


**Figure 20** Drilling Equipment for Injection Boreholes

The permeability of the grouted sealing blanket was tested before and after the injection by means of water permeability tests in accordance with the Lefranc method. Here, a defined volume (determined on drilling depth and drilling diameter) is sealed with a pneumatic packer and subjected to a constant hydrostatic pressure. The local permeability was calculated on the basis of the discharged subsoil water quantity over a certain amount of time. The construction site was divided into 20 equal sized sections, in which one to two tests were performed before and after the injection.
From the results of water tests, a reduction in permeability of about $2*10^{-4}$ m/s to $2*10^{-5}$ m/s could be determined. The remaining water inflow was in total 1.800m³/h. This amount is corresponding to a permeability of $2*10^{-5}$ m/s.


**Figure 21** Results of a Drill Core after Injection

### 5.4 Dewatering

In order to control groundwater levels and ensure almost dry conditions inside the construction pit the installation of an array of deep wells around the internal perimeter of the diaphragm wall shoring system and additional wells inside the pit area was installed. The in total 30 wells had a diameter of 600mm and were equipped with a PVC well casing of a diameter of 300mm. Since there are no standardized filter grains suitable for filter gravel in Saudi Arabia, various grains in different sizes were mixed on site in order to provide a suitable filter pack.


**Figure 22** Installation of the Gravel Filter at a Well

The extracted groundwater was passed through a ring line to the sedimentation basin.


**Figure 19** Results of a Drill Core after Injection

The pipe bridges commonly used in Germany are not common in Saudi Arabia. Underground pipes are standard here. The construction of a discharge line is therefore very complex. Here, the water was discharged over 2 pipelines DN800.

**Figure 24** Water Drainage in Operation

**Literatur:**


[L1] A. Mühl; K. Röder; C. Wawrzyniak: “Anwendung und Grenzen der numerischen Berechnung in der Geotechnik im Hinblick auf die Schnittstelle zur Hochbaustatik - Planung einer Pfahl-Platten-Gründung ”, Pfahl-Symposium 2013, Tagungsband S. 427-446,

[L2] ACI 318-08, Building Code Requirements For Structural Concrete

[L3] ASTM C1012, Standard Test Method for Length Change of Hydraulic-Cement Mortars Exposed to a Sulfate Solution


Authors


Dipl.-Ing. Alexander Mühl
alexander.muehl@cdmsmith.com
Dipl.-Ing. Michael Brunner
michael.brunner@cdmsmith.com
CDM Smith Consult GmbH
Weißenfelser Straße 65H www.cdmsmith.com
04229 Leipzig Tel.: 0341 333 89 580

Dr.-Ing. Christian Wawrzyniak
christian.wawrzyniak@cdmsmith.com
CDM Smith Consult GmbH
Motorstraße 5 www.cdmsmith.com
70499 Stuttgart Tel.: 0711 83 07 620